Short-chain fatty acids and ketones directly regulate sympathetic nervous system via GPR41

Ikuo Kimura[1], Daisuke Inoue[1], Takeshi Maeda[1], Takafumi Hara[1], Atsuhiko Ichimura[1], Satoshi Miyauchi[1], Makio Kobayashi[2], Akira Hirasawa[1] and Gozoh Tsujimoto [1*]

[1]Department of Genomic Drug Discovery Science, Kyoto University Graduate School of Pharmaceutical Sciences, Sakyo-ku, Kyoto 606-8501, Japan

[2]Department of Pathology, Tokyo Women's Medical University, 8-1, Kawada-cho, Shinjuku-ku, Tokyo 162-8666, Japan

Author Contributions: I.K. conceived the project, performed the experiments, interpreted data and wrote the paper. D.I. performed the experiments and interpreted data. D.Y., T.M., S.M. A.I and T.H. performed experiments. M.K., A.H. and H.T. performed interpreted data. G.T. supervised the project, interpreted data and wrote the paper.

*Address correspondence to: Gozoh Tsujimoto, M.D., Ph.D., Department of Genomic Drug Discovery Science, Kyoto University Graduate School of Pharmaceutical Sciences, Sakyo-ku, Kyoto 606-8501, Japan Tel: 81-75-753-4523, Fax: 81-75-753-4544; E-mail: gtsuji@pharm.kyoto-u.ac.jp

Abstract

The maintenance of energy homeostasis is essential for life, and its dysregulation leads to a variety of metabolic disorders. Under a fed condition, mammals utilize glucose as the main metabolic fuel, and short-chain fatty acids (SCFAs) produced by the colonic bacterial fermentation of dietary fiber also contribute a significant proportion of daily energy requirement. Under ketogenic conditions such as starvation and diabetes, ketone bodies produced in the liver from fatty acids are utilized as the main energy sources. In order to balance the energy intake, dietary excess and starvation triggers an increase or a decrease in energy expenditure, respectively, by regulating activity of the sympathetic nervous system (SNS). The regulation of metabolic homeostasis by glucose is well recognized; however, the roles of SCFAs and ketone bodies in maintaining energy balance remain unclear. Here, we show that SCFAs and ketone bodies directly regulate SNS activity via GPR41, a Gi/o protein-coupled receptor for SCFAs, at the level of sympathetic ganglion. GPR41 was most abundantly expressed in sympathetic ganglia in mouse and human. SCFA, propionate promoted sympathetic outflow via GPR41. On the other hand, a ketone body, β-hydroxybutyrate, produced during starvation or diabetes, suppressed SNS activity by antagonizing GPR41. Pharmacological and siRNA experiments indicated that GPR41-mediated activation of sympathetic neurons involves Gβγ-PLCβ-MAPK signaling. Sympathetic regulation by SCFAs and ketone bodies correlated well with their respective effects upon energy consumption. These findings establish that SCFAs and ketone bodies directly regulate GPR41-mediated SNS activity, and thereby control body energy expenditure in maintaining metabolic homeostasis.

Introduction

In order to balance the energy intake, dietary excess and fasting triggers an increase or a decrease in energy expenditure, respectively, by regulating activity of the sympathetic nervous system (SNS) (1-3) and its dysregulation leads to metabolic disorders such as obesity and diabetes (4, 5). In feeding, excessive energy is consumed by the enhancement of sympathetic function, resulting in increases in heart rate and diet-induced thermogenesis (2, 6), whereas in fasting, energy usage is saved by the suppression of sympathetic function as a survival mechanism, resulting in the reduction in heart rate and activity (3, 6). Under a fed condition, mammals utilize glucose as the main metabolic fuel, and short-chain fatty acids (SCFAs) produced by the colonic bacterial fermentation of dietary fiber also contribute a significant proportion of daily energy requirement (7, 8). Under ketogenic conditions such as fasting and diabetes, ketone bodies produced in the liver from fatty acids are utilized as the main energy sources (9, 10). However, effect of monocarboxylic metabolites, as SCFAs and ketone bodies, on the regulation of SNS activity remains unclear.

Free fatty acids (FFA) are not only essential nutrients but they also act as signaling molecules in various cellular processes. Recently, several groups reported that five orphan receptors, GPR40, GPR41, GPR43, GPR84, and GPR120, can be activated by FFAs. Long-chain fatty acids are specific agonists for GPR40 and GPR120 (11, 12) and medium-chain fatty acids for GPR84 (13). Short-chain fatty acids can activate GPR41 (14) and GPR43 (15). Stimulation of GPR41 by FFAs resulted in inhibiting cAMP production and activation of the ERK cascade, which suggests interactions with the Gα(i/o) family of G proteins (16, 17). GPR41 had been reported to be expressed in adipose tissue and promote secretion of leptin (18, 19). Other physiological functions of GPR41 still remain to be explored.

In the present study we show that SCFAs and ketone bodies, major energy sources in body, directly regulate sympathetic activity via GPR41. Examining the cardiac and metabolic sympathetic

responses *in vitro* as well as in mice lacking GPR41, we found that propionate (a major SCFA) and β-hydroxybutyrate (a major ketone body) promotes or depresses GPR41-mediated SNS activation, respectively.

Results

Abundant *Gpr41* expression in sympathetic ganglia and reduced sympathetic nerve activity in *Gpr41−/−* mice.

Examining *Gpr41* and *Gpr43* expression in tissues, we found that *Gpr41* was most abundantly expressed in the sympathetic ganglia such as the superior cervical ganglion (SCG) in adult mouse (Fig. 1*A*). SCG is an extension of the cervical sympathetic chain and a mass of sympathetic neurons. Compared with *Gpr41*, *Gpr43* was scarcely expressed in the SCG of either wild-type or *Gpr41−/−* mice (Fig. S1*A*, *B*). *In situ* hybridization revealed that *Gpr41* was most abundantly expressed in sympathetic ganglia and trunks during embryonic (E13.5 and 15.5), postnatal (P1) stages (Fig. 1*B*, *C*) to adulthood in mice, and also in the sympathetic ganglia of human adults (Fig. S1*C*, *D*).

To determine the effect of GPR41 on SNS, we generated *Gpr41−/−* mice (Fig. S2). *Gpr41−/−* mice exhibited normal growth and no major morphological abnormalities. Body weight, heart-weight/body-weight ratio and metabolic parameters and hormones (plasma concentrations of glucose, triglycerides, free fatty acids, leptin and insulin) were comparable between wild-type and *Gpr41−/−* mice (Fig. S3*A-G*). During development (P1), the SCG volume was significantly smaller in *Gpr41−/−* than wild-type mice (Fig. 1*D*, *E*). *Gpr41−/−* mice exhibited significantly reduced density of sympathetic innervations and tyrosine hydroxylase (TH) protein in the heart (Fig.1*F-H*), indicating that GPR41 may be involved in sympathetic nerve growth. TH is the rate-limiting enzyme for catecholamine biosynthesis, and plays an important role in the sympathetic regulation of the heart function. Corresponding with the retarded growth of sympathetic innervations, resting heart

rate was significantly reduced in *Gpr41−/−* mice (682 ± 10 beat/min and 610 ± 16 beat/min, in wild-type and *Gpr41−/−*, n = 12 each, respectively) (Fig. 2*B*). In *Gpr41−/−* mice, on the other hand, cardiac noradrenaline (NA) content was significantly increased, while plasma NA level was decreased (Fig. 2*A*). The reduction in heart rate associated with treatment using the β-adrenoceptor blocker propranolol was more marked in wild-type than *Gpr41−/−* mice, and the resultant heart rates were similar to both wild-type and *Gpr41−/−* mice (Fig. 2*B*). Treatment with tyramine, an agent causing release of stored NA from sympathetic nerve terminals, reduced heart rate, plasma and cardiac NA concentrations in both groups of mice, and the between-group differences in the parameters before tyramine treatment were not found (Fig. 2*C* and Fig. S3*H*). Results suggested that lower resting heart rate in *Gpr41−/−* mice is due to the reduced SNS activity. Furthermore, enhanced cardiac NA stores and the reduced circulating NA levels in *Gpr41−/−* mice indicated that GPR41 may contribute to NA release from SNS.

Effects of SCFA upon sympathetic activity.

In order to demonstrate that SCFAs are relevant for the effects of GPR41 upon SNS, we examined the effect of propionate, an SCFA found to have the most potent agonistic effect in heterologous expression system (Fig. S4). Administration of propionate (1 g/kg, i.p.), but not a middle-chain fatty acid octanoate (1 g/kg, i.p.), caused a significant increase in heart rate in wild-type and *Gpr43−/−* mice, whereas neither propionate nor octanoate caused any change in heart rate in *Gpr41−/−* mice (Fig. 2*D, E* and Fig. S5*A, B*). Also, metabolic parameters and hormones (plasma concentrations of glucose, triglycerides, free fatty acids and leptin) following administration of propionate were comparable between wild-type and *Gpr41−/−* mice (Fig. S5*C*). Treatment with a ganglion blocker hexamethonium (20 mg/kg i.p.) had little effect on this propionate-induced increase in heart rate, while propranolol (4 mg/kg i.p.) abolished the response (Fig. 2*F*). To confirm that the treatments

with hexamethonium and propranolol have respective ganglion blocking and β-blocking effects, we examined their effects on heart rate responses to a cholinergic agonist carbachol and β-adrenoceptor agonist isoproterenol. Carbachol- and isoproterenol- induced increases in heart rate were suppressed by hexamethonium and by propranolol, respectively (Fig. 2*F*). Thus, propionate may modulate the SNS activity at the level of sympathetic ganglion via GPR41 but not GPR43.

SCFA propionate induced sympathetic activation via GPR41-Gβγ in sympathetic neurons.

We further examined whether this propionate-induced positive chronotropism is due to the GPR41-mediated SNS activation or not, by using co-culture of primary-cultured fetal isolated cardiomyocytes and sympathetic neurons. RT-PCR assays confirmed that primary-cultured sympathetic neurons obtained from fetal SCG highly express *Gpr41*, but that fetal isolated cardiomyocytes lack *Gpr41* expression (Fig. S6*A*). In primary-cultured sympathetic neurons from wild-type and *Gpr43−/−* mice, propionate evoked extracellular action potentials (Fig. 3*A* and Fig. S6*B*). However, this propionate-activated response was not observed in sympathetic neurons obtained from *Gpr41−/−* mice (Fig. 3*A*). Propionate reduced intracellular cAMP concentrations and promoted ERK1/2 phosphorylation in primary-cultured sympathetic neurons (Fig. S6*C*, *D*). These propionate-induced responses were not observed in sympathetic neurons from *Gpr41−/−* mice, and they were abolished by pertussis toxin (PTX) (Fig. S6*C-E*), indicating that propionate-activated GPR41 signaling is required Gi/o. We further examined the effects of SCFAs on cardiac SNS activity by using the co-culture of fetal isolated cardiomyocytes with primary-cultured sympathetic neurons. Isoproterenol significantly increased beat rate in either mono-cultured or co-cultured cardiomyocytes. Propionate, on the other hand, reduced beat rate in mono-cultured cardiomyocytes, while in co-cultured cardiomyocytes propionate did not reduce, rather increased beat rate, which was abolished by propranolol (Fig. 3*B*). Therefore, propionate significantly ($p < 0.005$) increased beat

rate of the cardiomyocytes co-cultured with SCG neurons compared with that of the mono-cultured myocytes (Fig. 3*B*). As with wild-type mice, isoproterenol increased and propionate reduced beat rate, respectively, in mono-cultured cardiomyocytes isolated from *Gpr41−/−* mice (Fig. S6*F*). However, in co-culture of isolated cardiomyocytes with sympathetic neurons obtained from *Gpr41−/−* mice, propionate did not elicit a rise in beat rate (Fig. 3*C*). Rather, propionate reduced beat rate, as was observed in experiments with mono-cultured cardiomyocytes (Fig. 3*C*). Results showed that an SCFA propionate evokes action potentials in sympathetic neurons via GPR41, and thereby directly enhances SNS outflow. We further examined the GPR41-mediated signaling in SCG neurons. As G-protein signaling has been recently well characterized by using selective pharmacological tools (such as, inhibitors for Gα and Gβγ proteins), we adopted NF023 (Gα(i/o) blocker) and Gallein (Gβγ blocker) for the purpose (20, 21). GPR41-mediated generation of action potential and rise in beat rate was effectively blocked by Gallein and PTX treatment, while NF023 had no inhibitory effects (Fig. 3*D, E*). We confirmed that PTX and NF023 successfully inhibited GPR41-mediated cAMP inhibition, while Gallein had no such an inhibitory effect (Fig. S6*G*). These series of pharmacological studies showed that GPR41-mediated excitatory responses in SCG is mediated by Gβγ, but not by Gα(i/o) coupled to cAMP inhibition. We further examined the intracellular signaling for GPR41-induced sympathetic activation by using RNA interference. As it was difficult to transfer small interfering RNA (siRNA) into the primary cultured sympathetic neuron, we adopted mouse neuroblastoma cell line Neuro2A cells as a surrogate of sympathetic neurons (22, 23). Neuro2A cells express barely *Gpr41* or *Gpr43* (Fig. S6*H*). Propionate significantly increased beat rate when cardiomyocytes were co-cultured with Neuro2A cells expressing GPR41 (Fig. 3*F* and Fig. S6*I*). NGF, known to stimulate noradrenaline release from sympathetic neurons (24), increased beat rate when co-cultured with Neuro2A cells either transfected with or without *Gpr41* (Fig. 3*F*). Treatment of GPR41-expressing Neuro2A cells with siRNA for PLCβ2/3, but not

those for β-arrestin1/2 and GRK2 (25. 26), significantly inhibited the propionate-induced rise in beat rate of cardiomyocytes when co-cultured (Fig. 3*G* and Fig. S6*J, K*). Moreover, siRNA for ERK1/2, but not Gαq, showed a significant inhibitory effect (Fig. 3*G*). These results indicate that GPR41-activation of sympathetic neurons may involve Gβγ, PLCβ and MAPK, but not Gα(i/o), β-arrestin and GRKs.

A ketone body β-hydroxybutyrate inhibited sympathetic activity by antagonizing GPR41.

Under ketogenic conditions such as fasting, low-carbohydrate diet feeding, and diabetes, fatty acids and ketone bodies are utilized as the main energy sources (27). In assessing the effects of SCFAs and ketone bodies in GPR41-expressing HEK293 cells (16), we found that β-hydroxybutyrate has a potent antagonistic effect on GPR41, whereas acetoacetate, another major ketone body, has no significant effect (Fig. S7*A*). β-hydroxybutyrate suppressed propionate-induced ERK1/2 activation in a dose-dependent manner (Fig. 4*A*), and inhibited the propionate-induced reduction in cAMP production in GPR41-expressing HEK293 cells (Fig. 4*B*). β-hydroxybutyrate also inhibited both propionate-evoked firing frequency in primary-cultured sympathetic neurons (Fig. 4*C*), and propionate-induced rise in beat rate of cardiomyocytes co-cultured with sympathetic neurons (Fig. 4*D*). Administration of β-hydroxybutyrate (500 mg/kg, i.p.), but not another major ketone body acetone (0.5 g/kg, i.p.), caused a significant decrease in heart rate in wild-type mice, whereas either β-hydroxybutyrate or acetone caused less change in heart rate in *Gpr41−/−* mice (Fig. 4*E* and Fig. S7*B-E*). Moreover, β-hydroxybutyrate also inhibited the propionate-induced increase in heart rate in wild-type mice but not *Gpr41−/−* mice (Fig. 4*F*). Treatment with hexamethonium did not affect the β-hydroxybutyrate-induced decrease in heart rate, while propranolol completely suppressed the response (Fig. S7*F*). The results show that β-hydroxybutyrate may also inhibit the SNS activity at the level of sympathetic ganglion. Hence, it may be possible for β-hydroxybutyrate

to suppress the propionate-induced SNS activation as an antagonist for GPR41.

Reduced sympathetic activity under ketogenic conditions is partly due to GPR41 antagonism by β-hydroxybutyrate.

We further assessed the effect of β-hydroxybutyrate which can be endogenously produced under ketogenic conditions upon SNS activity. Following 48 hr starvation, metabolic parameters (body weight, and plasma levels of glucose, triglycerides and free fatty acids) were comparable between wild-type and *Gpr41−/−* mice (Fig. S8*A-D*). Plasma concentration of β-hydroxybutyrate was significantly higher in *Gpr41−/−* mice compared with wild-type mice (Fig. S8*E*). During fasting heart rate can be declined due to sympathetic depression (6, 10). The fasting-associated decline in heart rate was significantly lower in *Gpr41−/−* compared with wild-type mice (Fig. 5*A*). At 48 hr starvation an excessive increase in NA stores in the heart was observed in wild-type mice, which may reflect the decreased SNS activity; however, such an excessive increase in NA stores was not observed in *Gpr41-/-* mice (Fig. 5*B*). Further, the reduction in heart rate by propranolol was markedly smaller during starvation compared with fed conditions in wild-type mice (Fig. 5*C*). On the other hand, in *Gpr41-/-* mice the reduction in heart rate by propranolol was not affected by 48 hr starvation (Fig. 5*C*). Taken together, the results showed that starvation-associated sympathetic depression appears to be lacking in *Gpr41−/−* mice.

Ketone bodies increase dramatically in diabetes (10). In streptozotocin (STZ)-induced diabetes in mice, heart rate declined during the progression of diabetes (28). Reduction of heart rate in the diabetic condition was significantly smaller in *Gpr41−/−* compared with wild-type mice (Fig. 5*D*), although STZ-induced diabetic condition had similar effects on body weight, plasma levels of glucose and β-hydroxybutyrate in either group (Fig. S8*F*). Further, propranolol induced a significantly smaller reduction in heart rate in diabetics mice compared with control wild-type mice

(Fig. 5*E*). In *Gpr41−/−* mice, on the other hand, propranolol did not cause any effect upon heart rate, either with or without STZ treatment (Fig. 5*E*).

Collectively, our results indicate that GPR41 is required to induce sympathetic depression under ketogenic conditions, caused by either starvation or diabetes. However, the heart rate progressively decreased with time elapsed during ketogenic conditions in both WT and *Gpr41−/−* mice. Also, propranolol treatment decreased ~130 heart rates in WT mice (Fig. 5*C, E*), while ketogenic conditions decreased ~300 heart rates (Fig. 5*A, D*), respectively, indicating that ketone bodies not only inhibit sympathetic activity, but also may have direct inhibitory effect on the heart rate.

Effects of GPR41-mediated regulation of sympathetic activity upon energy expenditure.

We further assessed to what extent the observed effects of SCFAs and ketone bodies upon SNS activity affect energy expenditure. Oxygen consumption during feeding was significantly higher in wild-type mice than *Gpr41−/−* mice (Fig. 6*A*). The oxygen consumption was significantly decreased by treatment with tyramine and during starvation in wild-type mice, whereas these effects were not exhibited in *Gpr41−/−* mice (Fig. 6*A*). As total activity was comparable between wild-type and *Gpr41−/−* mice during feeding and starvation (Fig. 6*B*), the change in oxygen consumption of *Gpr41−/−* mice may be due to the metabolic effect but not physical activity. Also, the respiratory exchange ratio (RER) was comparable between wild-type and *Gpr41−/−* mice during feeding and starvation (Fig. 6*C*). Furthermore, body temperature and *Ucp1* expression in brown adipose tissue were significantly lower in *Gpr41−/−* compared with wild-type mice (Fig. 6*D, E*). As observed with changes in heart rate, propionate (1 g/kg, i.p.) increased and β-hydroxybutyrate (500 mg/kg, i.p.) decreased the oxygen consumption in wild-type mice, respectively. These responses were abolished by tyramine treatment (Fig. 6*F, G*). In contrast, neither propionate, β-hydroxybutyrate, nor tyramine treatment, caused any change in the oxygen consumption of *Gpr41−/−* mice. Moreover,

10

β-hydroxybutyrate inhibited the propionate-induced increase in the oxygen consumption (Fig. 6*H*). Our results indicate that the effects of SCFA and ketone bodies upon oxygen consumption, which reflect energy expenditure, were well correlated with changes in heart rate, indicating that both physiological responses are controlled by GPR41-mediated SNS activation.

Discussion

The high expression level of *Gpr41* in sympathetic ganglia indicates that GPR41 might play an important role in these cells. A series of *in vitro* and *in vivo* studies with *Gpr41−/−* mice showed that an SCFA propionate potently activates SNS at sympathetic ganglia. The mechanism of GPR41-mediated activation of sympathetic ganglion neurons is not mediated by cAMP inhibition, rather involves Gβγ and MAPK signaling. Furthermore, a major ketone body β-hydroxybutyrate antagonizes SCFA-GPR41 signaling, and thereby inhibits SNS. As SCFAs and ketone bodies reflect the nutrient conditions, these monocarboxylic metabolites appear to control energy balance by directly regulating GPR41-mediated sympathetic activation. The GPR41-SNS activation pathway may work as one of important physiological mechanisms for these metabolic fuels to regulate body energy balance.

Gpr41 had been reported to be expressed in adipose tissue in mouse (19) and humans (14), and stimulate leptin secretion (18, 19). Recent studies, however, have reported that *Gpr41* is not expressed in mouse adipose tissues (29-32). Our qRT-PCR analysis also found that *Gpr41* is not detected in mouse adipose tissues (Fig. S9). In contrast to *Gpr41*, we found that *Gpr43* are highly expressed in mouse adipose tissues by qRT-PCR (Fig. S9), confirming previous reports (28). As propionate can activate GPR43 (14), it is possible that propionate can affect SNS by GPR43-mediated effects on adipocytes, especially by secretion of leptin that can potently activate SNS (33). However, administration of propionate induced a similar extent of alterations in metabolic

parameters and leptin levels in wild-type and *Gpr41−/−* mice (Fig. S5*C*), showing that propionate-activated GPR43 responses in *Gpr41−/−* mice were similar to wild-type mice. The results further confirmed the previous reports that SCFAs can promote leptin secretion from the adipose not via GPR41 (29, 30). Taken together, the results showed that the effects of SCFAs on SNS activity may not be mediated by their effects on adipocytes from which adipocytokines such as leptin that can change sympathetic nerve activity can be secreted.

GPR41 is Gi/o-coupled GPCR and coupled to the inhibition of cAMP production (17). In general, Gi/o-coupled GPCRs work as an inhibitory system. However, our study shows that activation of GPR41 by SCFA excites the SCG neurons by generating action potential, and thereby releases noradrenaline from sympathetic nerve terminals, showing that GPR41 mediates an excitatory signaling. Recently, however, many excitatory responses in a variety of cell systems have been reported to be mediated by Gi/o-coupled GPCRs, and those responses were mediated via Gβγ but not Gα(i/o) (34-38). Our study with selective antagonists for Gα(i/o) and Gβγ also showed that GPR41-mediated excitation of SCG neurons is mediated by Gβγ signaling but not cAMP inhibition by Gα(i/o). Further, our siRNA experiments showed that GPR41-mediated activation of sympathetic neurons involves PLCβ and MAPK signaling, but not β-arrestin and GRKs signaling. Taken together, as the catecholamine release in neurons is regulated by MAPK signaling (39, 40) and Gβγ signaling activates MAPK signaling via PLCβ in Gi/o-coupled GPCRs (38), our results may indicate that GPR41-induced sympathetic activation involves Gβγ-PLCβ-MAPK signaling.

Under fed conditions, a substantial proportion of total dietary energy intake derives from SCFAs produced via the colonic fermentation of dietary fibers by gut microbiota (5 - 10 %) (41). Levels of SCFAs in the gastrointestinal tract vary significantly depending on the amount of non-digestible fiber in the diet, and also relate to the composition of the gut microbiota. Change in the amount and composition of gut microbiota have been implicated in cardiovascular diseases and obesity in

humans (42, 43). Ketogenic conditions have been suggested as a reason for the increased incidence of cardiac disorders (44, 45). Furthermore, SCFAs have recently been reported to profoundly affect inflammatory responses via the chemoattractant receptor GPR43 (15). As a plethora of physiological processes are regulated by SNS, SCFA–GPR41 interactions that regulate SNS could represent a central mechanism to account for the effects of diet, prebiotics and probiotics upon body homeostasis, and may represent new avenues for understanding and potentially manipulating physiology and disease.

Materials and Methods

RNA extraction, qRT-PCR, *in situ* hybridization, immunohistochemistry, animal and diabetic model, generation of HEK293 cells expressing mouse GPR41, cultures of sympathetic neurons, Neuro2A and cardiomyocytes, transfection and knockdown by siRNA, western blotting and cAMP determination, cardiographic recording, biochemical analyses, electrophysiological recording, indirect calorimetry, thermometry, and statistical analyses are described in *SI Materials and Methods*.

Reference

1. Tseng, Y. H., Cypess, A. M. & Kahn, C. R. (2010) Cellular bioenergetics as a target for obesity therapy. *Nat Rev Drug Discov.* 9:465-482.

2. Bachman, E. S. et al. (2002) betaAR signaling required for diet-induced thermogenesis and obesity resistance. *Science.* 297:843-845.

3. Young, J. B. & Landsberg, L. (1977) Suppression of sympathetic nervous system during fasting. *Science.* 196:1473-1475.

4. Symonds, M. E., Sebert, S. P., Hyatt, M. A. & Budge, H. (2009) Nutritional programming of the metabolic syndrome. *Nat Rev Endocrinol.* 5:604-610.

5. Cottrell, E. C. & Ozanne, S. E. (2007) Developmental programming of energy balance and the metabolic syndrome. *Proc Nutr Soc.* 66:198-206.

6. Landsberg, L. (2006) Feast or famine: the sympathetic nervous system response to nutrient intake. *Cell Mol Neurobiol.* 26:497-508.

7. Bergman, E. N. (1990) Energy contributions of volatile fatty acids from the gastrointestinal tract in various species. *Physiol Rev.* 70:567-590.

8. Flint, H. J. et al. (2008) Polysaccharide utilization by gut bacteria: potential for new insights from genomic analysis. *Nat Rev Microbiol.* 6:121-131.

9. Balasse, E. O. & Fery, F. (1989) Ketone body production and disposal: effects of fasting, diabetes, and exercise. *Diabetes Metab Rev.* 5:247-270.

10. Cahill, G. F. Jr. (2006) Fuel metabolism in starvation. *Annu Rev Nutr.* 26:1-22.

11. Itoh, Y. et al. (2003) Free fatty acids regulate insulin secretion from pancreatic beta cells through GPR40. *Nature.* 422:173-176.

12. Hirasawa, A. et al. (2005) Free fatty acids regulate gut incretin glucagon-like peptide-1 secretion through GPR120. *Nat Med..* 11:90-94.

13. Wang, J., Wu, X., Simonavicius, N., Tian, H. & Ling, L. (2006) Medium-chain fatty acids as ligands for orphan G protein-coupled receptor GPR84. *J Biol Chem*. 281:34457-34464.

14. Brown, A. J. et al. (2003) The Orphan G protein-coupled receptors GPR41 and GPR43 are activated by propionate and other short chain carboxylic acids. *J Biol Chem*. 278:11312-11319.

15. Maslowski, K. M. et al. (2009) Regulation of inflammatory responses by gut microbiota and chemoattractant receptor GPR43. *Nature*. 461:1282-1286.

16. Stoddart, L. A., Smith, N. J., Jenkins, L., Brown, A. J. & Milligan, G. (2008) Conserved polar residues in transmembrane domains V, VI, and VII of free fatty acid receptor 2 and free fatty acid receptor 3 are required for the binding and function of short chain fatty acids. *J Biol Chem*. 283:32913-32924.

17. Le, Poul. E. et al. (2003) Functional characterization of human receptors for short chain fatty acids and their role in polymorphonuclear cell activation. *J Biol Chem*. 278:25481-25489.

18. AI-Lahham, S. H. et al. (2010) Regulation of adipokine production in human adipose tissue by propionic acid. Eur J Clin Invest. 40:401-407.

19. Xiong, Y. et al. (2004) Short-chain fatty acids stimulate leptin production through the G protein-coupled receptor GPR41. *Proc Natl Acad Sci U S A*. 101:1045-1050.

20. Beindl, W. et al. (1996) Inhibition of receptor/G protein coupling by suramin analogues. *Mol Pharmacol.* 50:415-423.

21. Lehmann, D. M., Seneviratne, A. M. & Smrcka, A. V. (2008) Small molecule disruption of G protein beta gamma subunit signaling inhibits neutrophil chemotaxis and inflammation. *Mol Pharmacol.* 73:410-418.

22. Tremblay, R. G. et al. (2010) Differentiation of mouse Neuro2A cells into dopamine neurons. *J*

23. Brautigam, M. et al. (1984) Tetrahydrobiopterin and total biopterin content of neuroblastoma (N1E-115, N2A) and pheochromocytoma (PC-12) clones and the dependence of catecholamine synthesis on tetrahydrobiopterin concentration in PC-12 cells. *J Neurochem.* 42:390-396.

24. Lockhart, S. T., Turrigiano, G. G. & Birren, S. J. (1997) Nerve growth factor modulates synaptic transmission between sympathetic neurons and cardiac myocytes. *J Neurosci.* 17:9573-9582.

25. Rajagopal, S., Rajagopal, K. & Lefkowitz, R. J. (2010) Teaching old receptors new trick: biasing seven-transmembrane receptors. *Nat Rev Drug Discov.* 9:373-386.

26. Lefkowitz, R. J. & Shenoy, S. K. (2005) Transduction of receptor signals by beta-arrestins. *Science.* 308:512-517.

27. Fukao, T., Lopaschuk, G. D. & Mitchell, G. A. (2004) Pathways and control of ketone body metabolism: On the fringe of lipid biochemistry. *Prostaglandins Leukot. Essent. Fatty Acids.* 70:243-251.

28. Maeda, C. Y., Fernandes, T. G., Timm, H. B. & Irigoyen, M. C. (1995) Autonomic dysfunction in short-term experimental diabetes. *Hypertension.* 26:1100-1104.

29. Zaibi, M. S. et al. (2010) Roles of GPR41 and GPR43 in leptin secretory responses of murine adipocytes to short chain fatty acids. *FEBS Lett.* 584:2381-2386.

30. Hong, Y. H. et al. (2005) Acetate and propionate short chain fatty acids stimulate adipogenesis via GPCR43. *Endocrinology.* 146:5092-5099.

31. Samuel, B. S. et al. (2008) Effects of the gut microbiota on host adiposity are modulated by the short-chain fatty-acid binding G protein-coupled receptor, Gpr41. *Proc Natl Acad Sci U S A.* 105:16767-16772.

32. Oh, da. Y. et al. (2010) GPR120 is an omega-3 fatty acid receptor mediating potent anti-inflammatory and insulin-sensitizing effects. *Cell.* 142:687-698.

33. Myers, M. G. Jr., Munzberg, H., Leinninger, G. M. & Leshan, R. L. (2009) The geometry of leptin in the brain: more complicated than a asimple ARC. *Cell Metab.* 9:117-123.

34. Uezono, Y. et al. (2004) Involvement of G protein betagamma-subunits in diverse signaling induced by G(i/o)-coupled receptors: study using the Xenopus oocyte expression system. *Am J Physiol Cell Physiol.* 287:C885-C894.

35. Kim, J. A. et al. (2001) Role of pertussis toxin-sensitive G-proteins in intracellular Ca2+ release and apoptosis induced by inhibiting cystic fibrosis transmembrane conductance regulator (CFTR) Cl-channels in HepG2 human hepatoblastoma cells. *J Cell Biochem.* 81:93-101.

36. Rhie, D. J. et al. (2003) Endogenous somatostatin receptors mobilize calcium from inositol 1, 4, 5-trisphosphate-sensitive stores in NG108-15 cells. *Brain Res.* 975:120-128.

37. Fresco,P. et al. (2007) A2A adenosine-receptor-mediated facilitation of noradrenaline release in rat tail artery involves protein kinase C activation and betagamma subunits formed after alpha2-adrenoceptor activation. *Neurochem Int.* 51:47-56.

38. Albert, P. R. & Robillard, L. (2002) G protein specificity: traffic direction required. *Cell Signal.* 14:407-418.

39. Rosmaninho-Salgado, J. et al. (2007) Intracellular signaling mechanisms mediating catecholamine release upon activation of NPY Y1 receptors in mouse chromaffin cells. *J Neurochem.* 103:896-903.

40. Park, Y. S. et al. (2006) Activity-dependent potentiation of large dense-core vesicle release modulated by mitogen-activated protein kinase/extracellularly regulated kinase signaling. *Endocrinology.* 147:1349-1356.

41. Owira, P. M. & Winter, T. A. (2008) Colonic energy salvage in chronic pancreatic exocrine insufficiently. *J Parenter Enteral Nutr.* 32:63-71.

42. Vijay-Kumar, M. et al. (2010) Metabolic syndrome and altered gut microbiota in mice lacking

43. Turnbaugh, P. J. et al. (2006) An obesity-associated gut microbiome with increased capacity for energy harvest. *Nature*. 444:1027-1031.

44. Kuppermann, N. et al. (2008) Prolonged QT interval corrected for heart rate during diabetic ketoacidosis in children. *Arch Pediatr Adolesc Med.* 162:544-549.

45. Bank, I. M. et al. (2008) Sudden cardiac death in association with the ketogenic diet. *Pediatr Neurol.* 39:429-431.

Figure Legends

Fig. 1. Abundant *Gpr41* expression in sympathetic ganglia and reduced sympathetic nerve activity in GPR41-deficient mice. (*A*) *Gpr41* expression in postnatal mouse tissues (P49) measured by qRT-PCR (n = 3). SCG, superior cervical ganglion. Internal control: *18S* rRNA expression. (*B*) *Gpr41* mRNA localization in mouse embryos (E13.5 and E15.5) as determined by *in situ* hybridization using an ^{35}S-labeled antisense *Gpr41* RNA probe. Red grains (arrowhead) superimposed on a hematoxylin−eosin stained section indicate *Gpr41* mRNA localization. Scale bar = 5 mm. (*C*) *Gpr41* mRNA localization in postnatal day 1 (P1) mice (left). Anti-tyrosine hydroxylase (TH) immunostaining (brown) (right). Scale bar = 1 mm. (*D, E*) Anti-TH antibody immunostaining (brown) in SCG at P1. Total volume was measured by quantifying the TH-positive area (n = 6). (*F*) Whole-mount immunostaining of the heart with anti-TH antibodies (brown, above). High magnification view (below). Scale bar = 1 mm. (*G*) Quantitative analysis of TH+ nerve areas (n = 5). (*H*) TH protein expression (n = 6). β-actin (loading control). Mice were analyzed at 12 weeks of age (*F-H*). *$p < 0.05$; **$p < 0.005$.

Fig. 2. Effects of SCFA upon sympathetic activity via GPR41 in GPR41-deficient mice. (*A*)

Noradrenaline (NA) concentrations in hearts (n = 10) and plasma (n = 6). (*B*) Effects of propranolol upon heart rate in *Gpr41−/−* mice. Measurement of heart rate at 10 min after propranolol administration (i.p., n = 7-9). hatched bar, propranolol treated. (*C*) Effects of tyramine upon heart rate. Measurement of heart rate (n = 9) at 24 hr following tyramine injection (i.p.). hatched bar, tyramine treated. (*D*) Effects of propionate upon heart rate in *Gpr41−/−* mice (i.p., n = 5-7). (*E*) Effects of octanoate upon heart rate in *Gpr41−/−* mice. Measurement of heart rate at 20 min after octanoate administration (i.p., n = 4-5). (*F*) After pre-treated with hexamethonium (20 mg/kg) or propranolol (4 mg/kg) for 10 min, at time 0, a bolus of propionate (1 g/kg), carbachol (50 μg/kg) or isoproterenol (3 μg/kg) were administered intraperitoneally (n = 4-6). Data of was measured at time 20 min (propionate) and 3 min (carbachol and isoproterenol). Mice were analyzed at 12 weeks of age. *$p < 0.05$; **$p < 0.005$.

Fig. 3. SCFA-GPR41 signaling in sympathetic neurons. (*A*) Action potentials and firing frequency in *Gpr41−/−* sympathetic neurons following stimulation with propionate (10 mM) (n = 3-8). (*B*) Change in myocyte beating rate in sympathetic neurons with and without propionate (1 mM) treatment, and effects of propranolol (0.2 μM) (n = 5-6). Isoproterenol (10 μM) was used as a positive control. (*C*) Effects of propionate upon change in myocyte beating rate in *Gpr41−/−* cardiomyocytes and sympathetic neurons (n = 6-8). (*D*) Firing frequency in sympathetic neurons (n = 4-9) by propionate (10 mM) stimulation after pre-treatment with or without PTX (100 ng/ml), Gallein (10 μM) or NF023 (10 μM) for 2 hr. Carbachol (1 μM), cholinergic agonist, was used as a positive control. (*E*) Effects of propionate upon change in myocyte beat rate in cardiomyocytes and sympathetic neurons (n = 6-11). Cells were stimulated by propionate (1 mM) after pre-treatment with or without PTX (100 ng/ml), Gallein (10 μM) or NF023 (10 μM) for 1 hr. Isoproterenol (10 μM) was used as a positive control. (*F*) Effect of propionate (1 mM) and NGF (50 ng/ml) on the

beating rate of cardiomyocytes when co-cultured with Neuro2A cells either with or without transfecftion of *Gpr41* (n = 6). (*G*) Effects of siRNA on propionate-induced increase in the beating rate of cardiomyocytes when co-cultured with Neuro2A cells expressing GPR41 (n = 6). *$p < 0.05$; **$p < 0.005$.
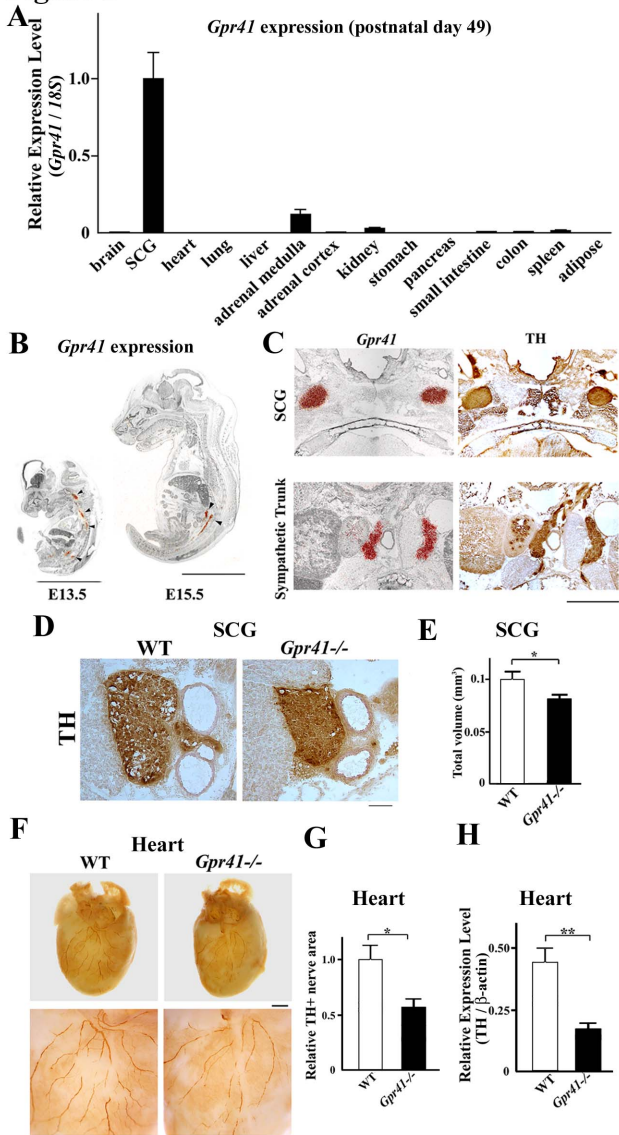
Fig. 4. Inhibitory effects of β-hydroxybutyrate to GPR41 upon sympathetic activity. (*A*) Antagonistic effects of β-hydroxybutyrate upon ERK1/2 phosphorylation by propionate (1 mM) in GPR41-expressing HEK293 cells (n = 3). (*B*) Reduction in cAMP levels in response to propionate (0.1 mM) treatment in GPR41-expressing HEK293 cells and inhibitory effects of β-hydroxybutyrate (100 mM) (n = 3). (*C*) Firing frequency in sympathetic neurons (n = 5) after propionate (10 mM) stimulation with or without β-hydroxybutyrate (10 mM). (*D*) Inhibitory effects of β-hydroxybutyrate (500μM) upon change in myocyte beat rate in cardiomyocytes and sympathetic neurons with propionate (1 mM) treatment (n = 5-8). (*E*) Effects of β-hydroxybutyrate upon heart rate of *Gpr41−/−* mice (500 mg/kg, i.p., n = 8). (*F*) Inhibitory effects of β-hydroxybutyrate upon heart rate of wild-type and *Gpr41−/−* mice. After pre-treated with β-hydroxybutyrate (500 mg/kg) for 10 min, at time 0, a bolus of propionate (1 g/kg) with or without β-hydroxybutyrate (500 mg/kg) was administered intraperitoneally (n = 5). Data was measured at time 20 min. Mice were analyzed at 12-14 weeks of age (*E*, *F*). *$p < 0.05$; **$p < 0.005$.

Fig. 5. Inhibitory effects of ketone bodies to GPR41 upon sympathetic activity during fasting or diabetes. (*A*) Heart rate following fasting in *Gpr41−/−* mice (n = 7-8). (*B*) NA content in the heart after 48 hr starvation (n = 9−10). (*C*) Effects of sympathetic nerve blocking upon heart rate of *Gpr41−/−* starved mice (n = 9-11). (*D*) Change in heart rate following the induction of diabetes (n = 4−10). (*E*) Effects of sympathetic nerve blocking upon heart rate in *Gpr41−/−* diabetic mice (n = 4,

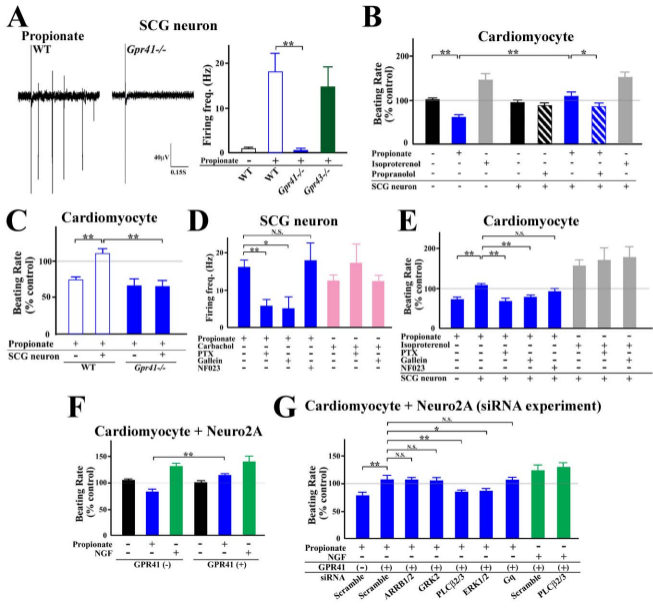5). Mice were analyzed at 12-14 weeks of age. *$p < 0.05$; **$p < 0.005$.

Fig. 6. Effects of GPR41-mediated regulation of sympathetic activity upon energy expenditure. (*A*) Effects upon oxygen consumption in *Gpr41−/−* mice during feeding and 48hr starvation. Measurement of oxygen consumption at 24 hr after tyramine administration (100 mg/kg, i.p.) (n = 5-7). (*B*) Total activity (24 hr) of *Gpr41−/−* mice during feeding and 24-48hr starvation (n = 9). (*C*) Respiratory exchange ratio (RER) of *Gpr41−/−* mice during feeding and 48hr starvation (n = 5-7). (*D*) Body temperature of *Gpr41−/−* mice during feeding (n = 6). (*E*) *Ucp1* expression in brown adipose tissue (BAT) in *Gpr41−/−* mice during feeding (n = 6). Internal control: *18S* rRNA expression. (*F*) Rate of oxygen consumption in propionate and PBS administration. Oxygen consumption was measured at 40 min after propionate administration (1 g/kg, i.p.) (n = 4-8). (*G*) Rate of oxygen consumption in β-hydroxybutyrate and PBS administration. Oxygen consumption was measured at 50 min after β-hydroxybutyrate administration (500 mg/kg, i.p.) (n = 5-7). Propionate and β-hydroxybutyrate were administrated after 24hr treatment of tyramine. Hatched bar, tyramine treated (*A*, *F*, *G*). (*H*) Inhibitory effects of β-hydroxybutyrate upon oxygen consumption. After pre-treated with β-hydroxybutyrate (500 mg/kg) for 10 min, at time 0, a bolus of propionate (1 g/kg) with or without β-hydroxybutyrate (500 mg/kg) was administered intraperitoneally (n = 8). Data was measured at time 40 min. Mice were analyzed at 14-16 weeks of age. *$p < 0.05$; **$p < 0.005$.
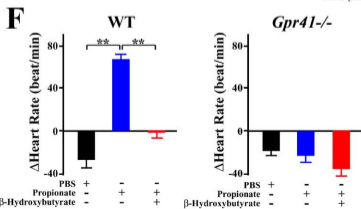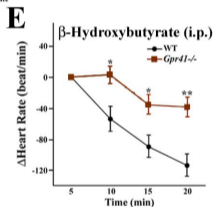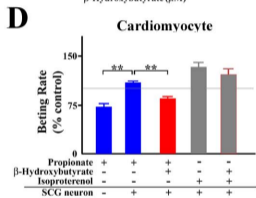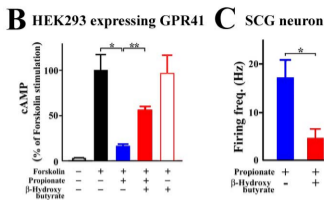
Figure 1

A — *Gpr41* expression (postnatal day 49)

Relative Expression Level (*Gpr41 / 18S*)

brain, SCG, heart, lung, liver, adrenal medulla, adrenal cortex, kidney, stomach, pancreas, small intestine, colon, spleen, adipose

B — *Gpr41* expression

E13.5   E15.5

C — *Gpr41*   TH

SCG

Sympathetic Trunk

D — SCG

WT   *Gpr41-/-*

TH

E — SCG

Total volume (mm³)

WT   *Gpr41-/-*

*

F — Heart

WT   *Gpr41-/-*

G — Heart

Relative TH+ nerve area

WT   *Gpr41-/-*

*

H — Heart

Relative Expression Level (TH / β-actin)

WT   *Gpr41-/-*

**

Figure 2

A Heart

Noradrenaline (pg/mg)

WT   *Gpr41-/-*

*

Plasma

Noradrenaline (pg/ml)

WT   *Gpr41-/-*

**

B Propranolol (i.p.)

Heart Rate (beat/min)

WT   *Gpr41-/-*

**

C Tyramine (i.p.)

Heart Rate (beat/min)

WT   *Gpr41-/-*

*

D Propionate (i.p.)

ΔHeart Rate (beat/min)

Time (min)

○ WT
■ *Gpr41-/-*
◆ *Gpr43-/-*

E Octanoate (i.p.)

ΔHeart Rate (beat/min)

WT   *Gpr41-/-*

F

ΔHeart Rate (beat/min)

Propionate
Carbachol
Isoproterenol
Hexamethonium
Propranolol

N.S.   *   **   **

Figure 3

Figure 4

A HEK293 expressing GPR41

P-ERK/ERK normalized by PMA

■ Propionate (+) □ Propionate (−)

β-Hydroxybutyrate (μM): 0, 0.1, 1, 10, 100, 1000

B HEK293 expressing GPR41

cAMP (% of Forskolin stimulation)

Forskolin
Propionate
β-Hydroxy-butyrate

C SCG neuron

Firing freq. (Hz)

Propionate
β-Hydroxy-butyrate

D Cardiomyocyte

Beting Rate (% control)

Propionate
β-Hydroxybutyrate
Isoproterenol
SCG neuron

E β-Hydroxybutyrate (i.p.)

ΔHeart Rate (beat/min)

● WT ■ Gpr41-/-

Time (min): 5, 10, 15, 20

F

WT

ΔHeart Rate (beat/min)

PBS
Propionate
β-Hydroxybutyrate

Gpr41-/-

ΔHeart Rate (beat/min)

PBS
Propionate
β-Hydroxybutyrate

Figure 5

Figure 6

SI Materials and Methods

RNA isolation and Real-time quantitative RT-PCR (qRT-PCR). Total RNA was extracted from tissues and cells using the RNeasy Mini Kit (Qiagen) and ISOGEN (WAKO). cDNAs were transcribed using RNAs as templates with Molony murine leukemia virus reverse transcriptase (Invitrogen). cDNAs were amplified by PCR with Taq DNA polymerase (TaKaRa) using primers shown in Supplementary Table 1. qRT-PCR analyses were performed using DNA Engine Opticon-2 (MJ Research) as described previously (1). For each condition, expression was quantified in duplicate.

In situ **hybridization.** For the *in situ* hybridization of histological sections, mouse embryos and human sympathetic ganglia were frozen in powdered dry ice, and 16 μm sections cut using a cryostat and stored at −80°C to await hybridization. ^{35}S-labeled mouse and human antisense *Gpr41* RNA probes were transcribed using T7 RNA polymerase with uridine 5′-α-[^{35}S]thio-triphosphate (Perkin Elmer). Sections were examined by *in situ* hybridization using a labeled probe, followed by exposure to X-ray films (Kodak) for 10 days as described previously (2). Sections were finally counterstained with hematoxylin–eosin.

Immunohistochemistry. For immunostaining, sections were fixed with 4% paraformaldehyde, washed in phosphate-buffered saline (PBS), and treated with 5% bovine serum albumin (BSA) in PBS. The sections were permeabilized with 0.1% Triton X-100 (Sigma) and immunostained with a primary antibody raised against tyrosine hydroxylase (TH, Chemicon) to detect sympathetic neurons. Sections and whole hearts were stained with an antibody to TH. Following hybridization with the secondary antibody, tissue samples were incubated with DAB. Total volumes of SCG and nerve area were measured by ImageJ software as described previously (2, 3). The volume of SCG was

estimated according to Cavalieri's principle.

Animal and diabetic model. All experimental procedures involving mice were carried out according to protocols approved by the relevant Animal Ethics Committees. *Gpr41-/-* and *Gpr43-/-* mice from a C57BL/6 background were generated. Type I diabetes was induced by an intraperitoneal (i.p.) injection containing streptozotocin (STZ) (Sigma, 200 mg/kg). STZ was dissolved in cold citrate buffer (50 mM; pH 4.5) immediately before injection. Glucose levels were measured from tail vein blood 4 days post-injection with a glucometer (Lifescan). Mice with blood glucose levels > 200 mg/dl were considered diabetic as described previously (4).

Generation of HEK293 cells expressing mouse GPR41. Flp-In T-REx HEK293 cells were transfected with a mixture containing mouse FLAG-GPR41 cDNA in pcDNA5/FRT/TO vector and the pOG44 vector using Lipofectamine (Invitrogen). After 48 hr, the medium was changed to medium supplemented with 200 μg/ml hygromycin B to initiate selection of stably transfected cells. Following isolation of resistant cells, expression of GPR41 from the Flp-In locus was induced by treatment with 1 μg/ml doxycycline for 48 hr as described previously (5). Expression of GPR41 was confirmed by RT-PCR and FACS Calibur (BD Biosciences) using FLAG-tag.

Cultures of sympathetic neurons, Neuro2A and cardiomyocytes. SCG was dissected from postnatal day 1 mice and trypsinized in 0.05% trypsin in Hanks' balanced salt solution for 20 min at 37°C, and dissociated by trituration. Dissociated cultures of SCG neurons were plated onto poly-L-lysine (20 μg/ml; Sigma) coated dishes in DF medium (Gibco) containing 1% penicillin–streptomycin solution (Gibco). The cells were cultured in conditioned medium containing NGF (10 ng/ml; Upstate Biotech) and 10% FBS (EQUITECH-BIO INC.) as described (6). Neuro2A

cells were cultured in DF medium (Gibco) containing 1% penicillin–streptomycin solution (Gibco) and 10% FBS (EQUITECH-BIO INC.) as described (6). For co-culture of SCG neurons and cardiac ventricular myocytes, freshly isolated sympathetic neurons were plated with cardiomyocytes obtained from the same animals and cultured for 2 days before analysis as described (6). Cells were cultured using the same methods as cultures of SCG neurons. After 1 day in culture, 1 mM cytosine arabinofuranoside (Sigma) was added to the dishes to stop cell division. For co-culture of Neuro2A neurons and cardiomyocytes, Neuro2A cells were cultured in DF containing 1% N2 Supplement (Gibco) for neuronal differentiation for 24 hr before plating with cardiomyocytes.

Transient transfection and knockdown by siRNA.

For Gpr41 overexpression, Neuro2A cells were transfected with mouse FLAG-GPR41 cDNA in pcDNA3.1 vector using Lipofectamine 2000 (Invitrogen). After 24 hr, for RNA interference, Neuro2A cells were transfected with 40nM siRNA shown in Supplementary Table 2 (Stealth Select RNAi, Invitrogen) by using the Lipofectamine RNAiMAX transfection reagent (Invitrogen) as described (7). The transfected cells were cultured in DF containing 10% FBS for 24 hr and then in DF containing 1% N2 Supplement (Gibco) for neuronal differentiation.

Western blotting and cAMP determination. Cells were first lysed in TNE buffer. Hearts were homogenized in 0.1 M sodium phosphate (pH 7.4) and were centrifuged at 10,000g for 20 min at 4°C. Supernatants were analyzed by Western blotting and proteins detected by Western blotting using the following antibodies: rabbit antibodies against ERK1/2, phosphorylated ERK1/2, ARRB1/2, GRK2, PLCβ3 (Cell signaling), Gq (Santa Cruz), TH (Chemicon) and a mouse antibody against β-actin (Sigma). After transfer to nitrocellulose membranes, immunoreactive bands were visualized using an enhanced chemiluminescence detection system as previously described (5, 7).

For cAMP determination, the cells were lysed 0.1N HCl solution. After acetylation, cAMP level was determined in duplicate using Enzyme Immunoassay Kits (Cayman) as described (8).

Cardiographic recording. Heart rates were measured in conscious male mice using a tail-cuff system (Softron Co. Ltd.) as described (9). For measurement of physiological parameters, under resting conditions, propranolol (4 mg/kg), a β-adrenergic receptor antagonist, atropine (8 mg/kg), a muscarinic receptor antagonist, a hexamethonium (20 mg/kg), a nicotinic acetylcholine receptor antagonist, propionate (1 g/kg), octanoate (1 g/kg), β-hydroxybutyrate (500 mg/kg), acetone (0.5 g/kg) and tyramine (100 mg/kg), catecholamine releasing agent, were administrated at a volume per injection intraperitoneally (i.p.) as described (10, 11, 12). Atropine was injected first, and followed 10 min later by propranolol.

Biochemical analyses. Noradrenaline concentrations in Plasma and heats were measured by HPLC as described (3). Plasma glucose concentrations were measured using a glucometer (LifeScan). Plasma propionate, acetone and octanoate concentrations were measured by GC. Plasma β-hydroxybutyrate concentrations were measured using ketone test B liquid (SANWA). Measurements of plasma free fatty acids and triglyceride concentrations were entrusted to SRL Inc. Plasma leptin concentrations were measured using Leptin Mouse ELISA Kit (R&D Systems).

Electrophysiological recording. Extracellular action potentials were recording using a multichannel recording system (MED64 system; Alpha MED Sciences Co.). SCG neurons were plated onto poly-L-lysine coated MED probes and cultured in DF containing 10% FBS and NGF (10 ng/ml). Cells were starved in serum-free medium for 2hr before stimulation. Frequency was measured using Conductor software v.2.1e (Alpha MED sciences Co.) as described (13).

Indirect calorimetry. Oxygen consumption (VO_2) was determined with an O_2/CO_2 metabolic measuring system (Model MK-5000, Muromachikikai) at 24°C as described elsewhere (14). Mice were kept unrestrained in the chamber for 1 hr at three times without food and water. We determined VO_2 when the minimum plateau shape was obtained during the light cycle, which corresponded to a period of inactivity. VO_2 was expressed as the volume of O_2 consumed per kilogram weight of lean body mass per minute.

Thermometry

The body temperatures of the conscious mice were measured with life chip by using Pocket Reader (Destron Fearing). The life chip was placed in subcutaneous of the anesthetized mice. After implantation of the life chip, mice were allowed to recover for at least 24 hr before data collection.

Statistical analyses. Values are presented as mean ± standard error of the mean (s.e.m.). Differences between groups were examined for statistical significance using Student's t-test (when two groups were analyzed) or ANOVA (for three or more groups). P values of < 0.05 were considered statistically significant.

1. Kimura, I. et al. (2010) Neuferricin, a novel extracellular heme-binding protein, promotes neurogenesis. *J Neurochem.* 112, 1156-1167.

2. Ieda, M. et al. (2007) Sema3a maintains normal heart rhythm through sympathetic innervation patterning. *Nat Med.* 13:604-612.

3. Bishop, T. et al. (2008) Abnormal sympathoadrenal development and systemic hypotention in PHD3-/- mice. *Mol Cell Biol.* 28:3386-3400.

4.   Rose, K. L., Pin, C. L., Wang, R. & Fraser, D. D. (2007) Combined insulin and bicarbonate therapy elicits cerebral edema in a juvenile mouse model of diabetic ketoacidosis. *Pediatr Res.* 61:301-306.

5.   Hirasawa, A. et al. (2005) Free fatty acids regulate gut incretin glucagon-like peptide-1 secretion through GPR120. *Nat Med..* 11:90-94.

6.   Yang, B., Slonimsky, J. D. & Birren, S. J. (2002) A rapid switch in sympathetic neurotransmitter release properties mediated by the p75 receptor. *Nat Neurosci.* 5:539-545.

7.   Kimura, I. et al. (2008) Neurotrophic activity of neudesin, a novel extracellular heme-binding protein, is dependent on the binding of heme to its cytochrome b5-like heme/steroid-binding domain. *J Biol Chem.* 283:4323-4331.

8.   Hiroyama, M. et al. (2007) Hypermetabolism of fat in V1a vasopression receptor knockout mice. *Mol Endocrinol.* 21:247-258.

9.   Koshimizu, T. A. et al. (2006) V1a vasopressin receptors maintain blood pressure by regulating circulating blood volume and baroreflex sensitivity. *Proc Natl Acad Sci U S A.* 103:7807-7812.

10. Altman, J. D. et al. (1999) Abnormal Regulation of the Sympathetic Nervous System in α2A-Adrenergic Receptor Knockout Mice. *Mol Pharmacol.* 56:154-161.

11. Habecker, B. A. et al. (2008) Regulation of cardiac innervation and function via the p75 neurotrophin receptor. *Auton Neurosci.* 140:40-48.

12. Wallukat, G., Morwinski, R. & Kuhn, H. (1994) Modulation of the beta-adrenergic response of cardiomyocytes by specific lipoxygenase products involves their incorporation into phosphatidylinositol and activation of protein kinase C. *J Biol Chem.* 269:29055-29060.

13. Matsuda, S. et al. (2008) Microtubule-associated protein 2-positive cells derived from microglia possess properties of functional neurons. *Biochem Biophys Res Commun.* 368:971-976.

14. Oike, Y. et al. (2005) Angiopoietin-related growth factor antagonizes obesity and insulin

Supplementary Figure Legends

Fig. S1. *Gpr41* mRNA expression in the sympathetic ganglia.

(*A, B*) *Gpr41* and *Gpr43* expression in SCG of wild-type and *Gpr41−/−* mice (P49). Quantification of *Gpr41* and *Gpr43* expression was performed by qRT-PCR (n = 3). (*C*) Expression of *Gpr41* mRNA in human tissues. Expression of *Gpr41* was measured using qRT-PCR. *18S* rRNA expression was used as an internal control. (*D*) *Gpr41* mRNA localization in human abdominal sympathetic ganglia as determined by *in situ* hybridization using an ^{35}S-labeled antisense human *Gpr41* RNA probe. Red grains (arrowhead) superimposed on a hematoxylin−eosin stained section show *human Gpr41* mRNA localization. Anti-tyrosine hydroxylase (TH) immunostaining (brown) (right). Scale bar = 1 mm.

Fig. S2. Targeted disruption of *Gpr41* in mice. (*A*) A targeting vector was constructed by ligation of three fragments, the 5' and 3' homology recombination arms and a fragment of the LacZ-PGK-neo cassette. A 1.7-kbp fragment of mouse DNA containing the exon coding for *Gpr41* was replaced with the LacZ-PGK-neo cassette. The linearized targeting vector was then electroporated into 129/Sv ES cells. (*B*) The 3' probe used for Southern blotting is indicated below the map of the target allele. The 7.5-kbp and 3.5-kbp fragments, which correspond to the wild-type and mutant alleles, respectively, were detected from the genomic DNA digested with *Eco RV* and *Hpa I* by Southern blotting. **c,** Genotypes of mice were determined by PCR using the three primers, P1, P2, and P3 (wild-type (1.9-kbp, P1/P3) and mutant (1.3-kbp, P1/P2) alleles). P1: 5'-GCAGCAGAGTGCCAGTTGTCC-3', P2: 5'-GGCTATTCGGCTATGACTGG-3', P3: 5'-GCGTGTGAGTGGTCCTTCCATCC-3'

Fig. S3. Metabolic parameters of *Gpr41-/-* mice and NA concentration. (*A*) Body weights of wild-type mice and *Gpr41−/−* mice (n = 12). (*B*) Ratio of heart weights to body weights in wild-type mice and *Gpr41−/−* mice (n = 10). (*C-G*) Biochemical analysis of plasma obtained from *Gpr41−/−* mice (**c,** Glucose (n = 9); (*D*) Triglycerides (n = 9); (*E*) Free fatty acids (n = 9); (*F*) Leptin (n = 5); (*G*) Insulin (n = 6)). (*H*) Effects of tyramine upon NA concentrations. Measurement of NA concentrations in heart (n = 12) and plasma (n = 10) at 24 hr after tyramine injection (i.p.). Mice were analyzed at 12 weeks of age.

Fig. S4. Propionate as the most potent agonist for GPR41. Screening of GPR41 agonists by the phosphorylation of ERK1/2 assay in HEK293 cells expressing mouse GPR41. Monocarboxylates were added 1 mM, respectively for 5 min (n = 3). $*p < 0.05$; $**p < 0.005$.

Fig. S5. Effects of propionate upon heart rate. (*A*) At time 0, a bolus of propionate (1 g/kg) was administered intraperitoneally (n = 5) (left). The concentration of propionate in plasma following the injection of propionate (1 g/kg) (n = 3) (right). (*B*) The concentration of octanoate in plasma following the injection of octanoate (1 g/kg) (n = 3). (*C*) At 20 min after administration of propionate (1 g/kg, i.p.), biochemical analysis of plasma obtained from *Gpr41−/−* mice (Glucose (n = 5-6), Triglycerides (n = 5-6), Free fatty acids (n = 5-6), Leptin (n = 5)). (*D*) After pre-treated with or without hexamethonium (20 mg/kg) or propranolol (4 mg/kg) for 10 min, at time 0, a bolus of carbachol (50 μg/kg) or isoproterenol (3 μg/kg) were administered intraperitoneally (n = 4). Data was measured at 3 min. Mice were analyzed at 12 weeks of age. $*p < 0.05$; $**p < 0.005$.

Fig. S6. Effects of propionate in primary-cultured sympathetic neurons and Neuro2A cells. (*A*)

Expression of *Gpr41* mRNA in mono-cultured cardiomyocytes and co-cultured cardiomyocytes. (*B*) Action potentials in sympathetic neurons after propionate (10 mM) or PBS stimulation. (*C*) Reduction of cAMP levels in response to propionate in sympathetic neurons. Cells were stimulated by propionate (1 mM) in the presence of IBMX for 10 min (n = 5). (*D*) Effects of propionate on ERK1/2 phosphorylation. Sympathetic neurons stimulated by propionate (1 mM) for 30 min (n=3). (*E*) Effects of propionate on phosphorylation of ERK1/2. Sympathetic neurons were stimulated by propionate (1 mM) in the presence or absence of PTX (100 ng/ml) for 30 min. (*F*) Effects of propionate (1 mM) or isoproterenol (10 μM) upon change in myocyte beating rate in *Gpr41−/−* cardiomyocytes (n = 6-7). (*G*) Reduction of cAMP levels in response to propionate in HEK293 cells expressing mouse GPR41. Cells were stimulated by propionate (10 μM) in the presence of IBMX for 10 min after pre-treatment with IBMX for 30min and with or without PTX (1 μg/ml), Gallein (10 μM) or NF023 (20 μM) for 1 hr (n = 3). (*H*) *Gpr41* and *Gpr43* expression in Neuro2A cells and sympathetic neurons. Quantification of *Gpr41* and *Gpr43* expression was performed by qRT-PCR (n = 3). (*I*) Efficiency of *Gpr41* transient transfection in Neuro2A cells. Expression of *Gpr41* mRNA or GPR41 protein was measured using qRT-PCR (n = 3) or Western-blotting by anti-FLAG antibody. *18S* rRNA and β-actin expression were used as an internal control. (*J*) Knockdown efficiencies of siRNA knockdown in Neuro2A cells. Expression of *Arrb1, Arrb2, Grk2, Plcb2, Plcb3, Erk1, Erk2 and Gq* were measured using qRT-PCR. *18S* rRNA expression was used as an internal control. (*K*) Effects of knockdown by siRNA on protein expression in Neuro2A cells. Expression of ARRB1/2, GRK2, PLCβ3, ERK1/2 and Gq were measured using Western-blotting. β-actin expression was used as an internal control. *$p < 0.05$; **$p < 0.005$.

Fig. S7. β-hydroxybutyrate as GPR41 antagonist. (*A*) Effect of monocarboxylates on propionate-induced phosphorylation of the ERK1/2 in HEK293 cells expressing mouse GPR41.

After pretreatment of monocarboxylates (1mM each) or PBS for 10 min, cells were stimulated with propionate (1mM). Control: no pretreated and PBS stimulation. Effect of monocarboxylates on propionate-induced GPR41 stimulation was examined by quantifying P-ERK/ERK. (*B*) At time 0, a bolus of β-hydroxybutyrate (500 mg/kg) was administered intraperitoneally (n = 4). (*C*) The concentration of β-hydroxybutyrate in plasma following the injection of β-hydroxybutyrate (500 mg/kg) (n = 3). (*D*) Effects of acetone on heart rate in *Gpr41−/−* mice. Measurement of heart rate at 20 min after acetone administration (i.p., n = 6). (*E*) The concentration of acetone in plasma following the injection of acetone (0.5 g/kg) (n = 3).

Fig. S8. Metabolic parameters of *Gpr41−/−* mice in starvation and STZ-induced diabetes. (*A*) Body weights of *Gpr41−/−* mice after 48 hr starvation (n = 10-12). (*B-E*) Biochemical analysis of plasma obtained from *Gpr41−/−* mice after 48 hr starvation (*B*, Glucose (n = 9) *C,* Triglycerides (n = 9) *D,* Free fatty acids (n = 9−11) *E,* Ketone bodies, β-hydroxybutyrates (n = 8)). (*F*) Cardiographic and biochemical parameters in streptozotocin-induced diabetic *Gpr41−/−* mice (n = 7). All parameters were measured after the fourth day of STZ injection. Mice were analyzed at 12 weeks of age (*A-F*). $*p < 0.05$; $**p < 0.005$.

Fig. S9. *Gpr41* and *Gpr43* expression in adipose (mesenteric) of wild-type mice (P49). Quantification of *Gpr41* and *Gpr43* expression was performed by qRT-PCR (n = 3).

Table S1. Primers used for qRT-PCR assays.

Primer	Forward	Reverse
Gpr41 (mouse)	5'-GTGACCATGGGGACAAGCTTC-3'	5'-CCCTGGCTGTAGGTTGCATT-3'

18S (mouse)	5'-CTCAACACGGGAAACCTCAC-3'	5'-AGACAAATCGCTCCACCAAC-3'
Gpr43 (mouse)	5'-GGCTTCTACAGCAGCATCTA-3'	5'-AAGCACACCAGGAAATTAAG-3'
Gpr41 (human)	5'-CACTATGGATTGGGCTCTGG-3'	5'-TCTGCCACCCTCAAGAAAAC-3'
18S (human)	5'-AAACGGCTACCACATCCAAG-3'	5'-CGCTCCCAAGATCCAACTAC-3'
Ucp1 (mouse)	5'-GGCATTCAGAGGCAAATCAG-3'	5'-AGCATTGTAGGTCCCCGTG-3'
Arrb1 (mouse)	5'-CACGTCACCAACAACACCAAC-3'	5'-CGATGATGCCCAGGATTTCAC-3'
Arrb2 (mouse)	5'-GGAACTCTGTGCGGCTTATC-3'	5'-GAAGTGGCGTGTGGTTTCAG-3'
Grk2 (mouse)	5'-TCTTCCAGCCATACATTGAGG-3'	5'-GCAGAACCGTGTGAACTTGTC-3'
Plcb2 (mouse)	5'-ATGCTGGATGTCAGATGGTTG-3'	5'-TCGTAATGGAAAGGGTGGTGG-3'
Plcb3 (mouse)	5'-TGCCTGCCCTGCTTATCTAC-3'	5'-AGCCTCACTCTCCCCAATGA-3'
Erk1 (mouse)	5'-TATCAACACCACCTGCGACC-3'	5'-CATACTCCGTCAGAAAGCCAG-3'
Erk2 (mouse)	5'-CTCTCCCGCACAAAAATAAGG-3'	5'-TGGGCTCATCACTTGGGTC-3'
Gq (mouse)	5'-TGGAGAAGGTGTCTGCTTTTG-3'	5'-ATTCCCGTCGTCTGTCGTAG-3'

Table S2. siRNA used for RNAi.

siRNA	Sequence
Arrb1 #1	5'-UUCCCAGGUAGACAGUGAGCUUUCC-3'
Arrb1 #2	5'-UUUGGCGGGAUCUCAAAGGUGAAGG-3'
Arrb1 #3	5'-AUACAAUGUCGUCAUCAUUGGUGUC-3'
Arrb2 #1	5'-CAAACACGAUGUCAUCGUCUGUGGC-3'
Arrb2 #2	5'-UCAUGUUUGAGCUGCCCAUCCAAGG-3'
Arrb2 #3	5'-AGAACGUGGAACUAGGAGACACCUG-3'
Grk2 #1	5'-AACAAGUAGAAGUAUCGCCGCUGCC-3'

Grk2 #2	**5'-AUUCGAUGCACACUGAAGUCAUUCA-3'**
Grk2 #3	**5'-ACUAUCACACUGCAGGACAAACUGC-3'**
Plcb2 #1	**5'-UUCAGUUCCCGCAACUCUUCCAAGC-3'**
Plcb2 #2	**5'-UGAAGUUUCAUCGUCCCACUUGAUG-3'**
Plcb2 #3	**5'-UCAAGAUCUUCUCAAAGAUAAAGGG-3'**
Plcb3 #1	**5'-AUUUGAUGAACUUACUCCCGCGCCG-3'**
Plcb3 #2	**5'-UUCGCAGGCAGACAUAGUGGUAUCC-3'**
Plcb3 #3	**5'-UAAUCAAGGCCUCCGCAUAGUCCUG-3'**
Erk1 #1	**5'-UUGAUAAGCAGAUUGGAAGGCUUCA-3'**
Erk1 #2	**5'-UUUGGAGUCAGAUUUAGGAAAGAGC-3'**
Erk1 #3	**5'-AAUGUAAACAUCUCUCAUGGCUUCC-3'**
Erk2 #1	**5'-UCAUGAUCUGGAUCUGCAACACGGG-3'**
Erk2 #2	**5'-AUAAUACUGCUCCAGGUAUGGGUGG-3'**
Erk2 #3	**5'-UUAGCUGAAUGGAUAUACUUUAGCC-3'**
Gq #1	**5'-UUGUUGUGUAGGCAGAUAGGAAGGG-3'**
Gq #2	**5'-AAAUGACACUUUGUAAGUCAAAGGG-3'**
Gq #3	**5'-AGAACUUGAUCAUAUUCGCUAAGCG-3'**

Supplementary Figure 1

A — WT — mRNA expression in SCG (fM) — *Gpr41*, *Gpr43*

B — *Gpr41-/-* — mRNA expression in SCG (fM) — *Gpr41*, *Gpr43*

C — Relative Expression Level (*human Gpr41 / 18S*) — brain, heart, liver, sympathetic ganglia (abdominal), kidney, colon

D — Sympathetic ganglia (abdominal) — *human Gpr41* — TH
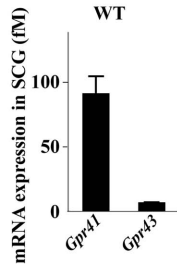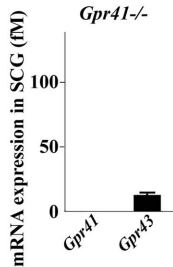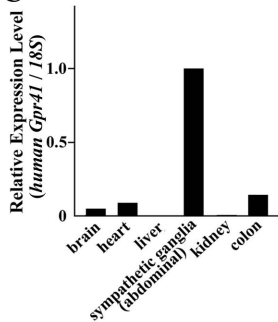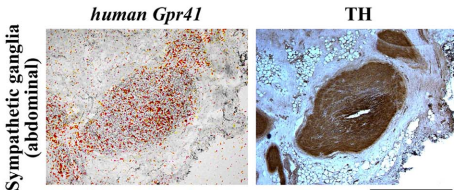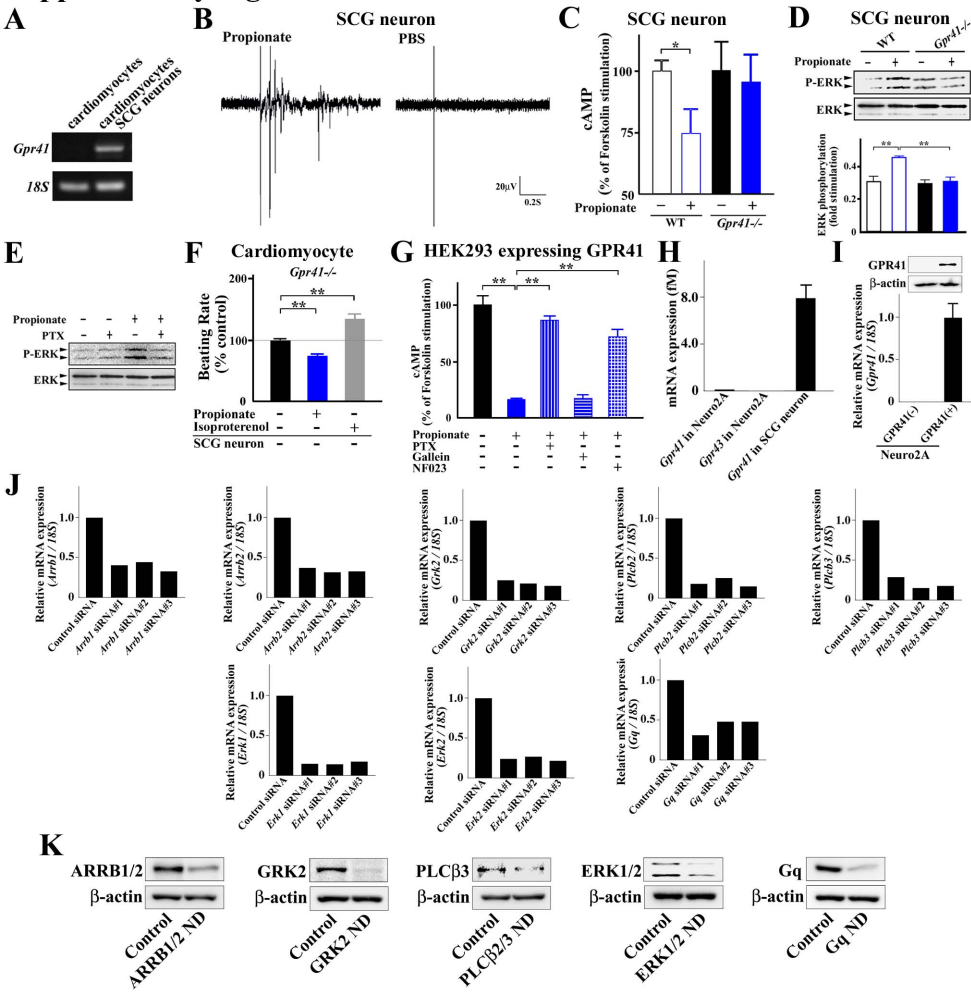
Supplementary Figure 2
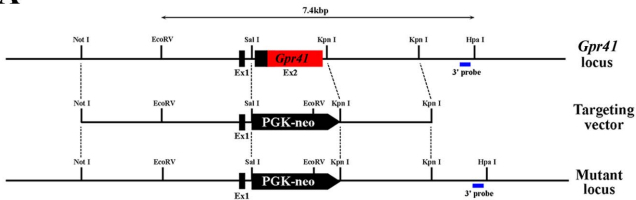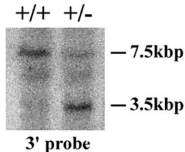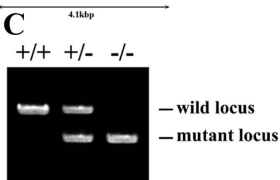
Supplementary Figure 3
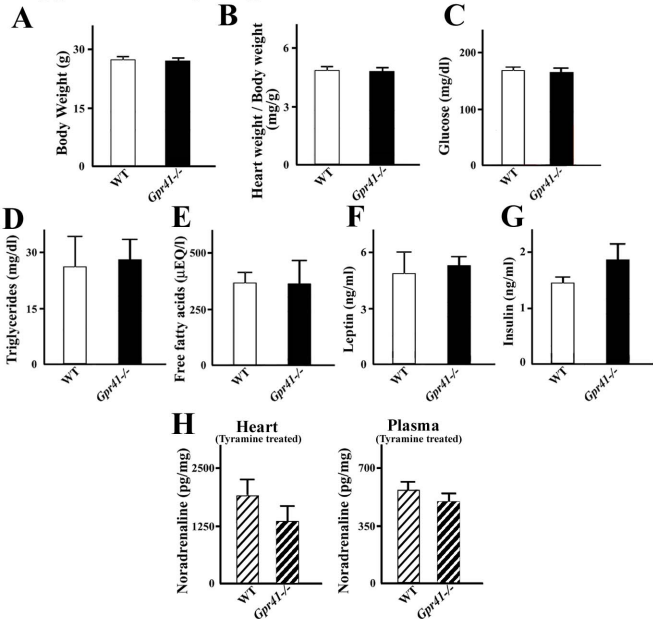
Supplementary Figure 4
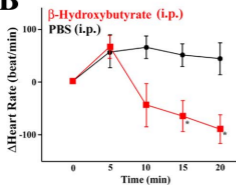

HEK293

P-ERK

ERK
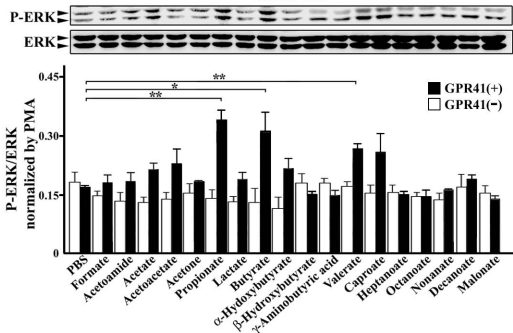
Supplementary Figure 5
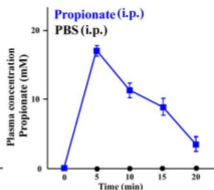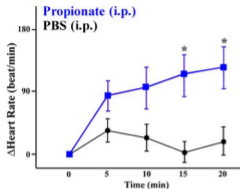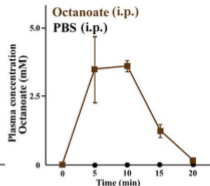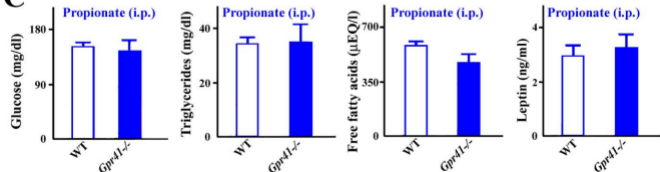
Supplementary Figure 6
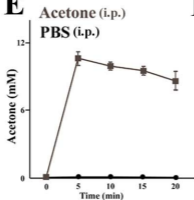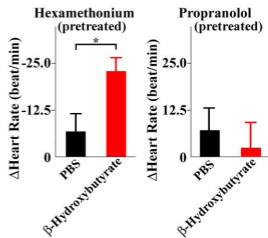
Supplementary Figure 7

A HEK293 expressing GPR41
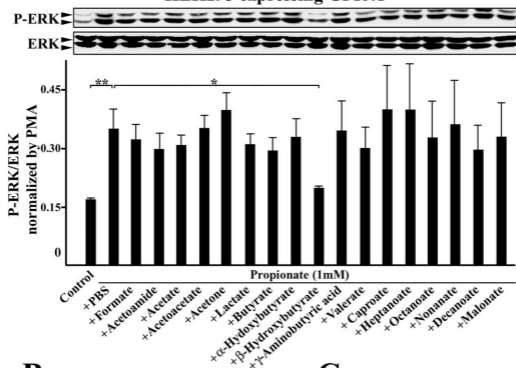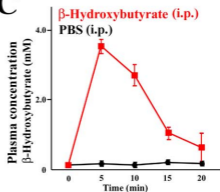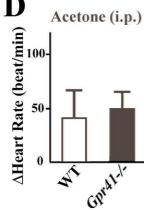
Supplementary Figure 8
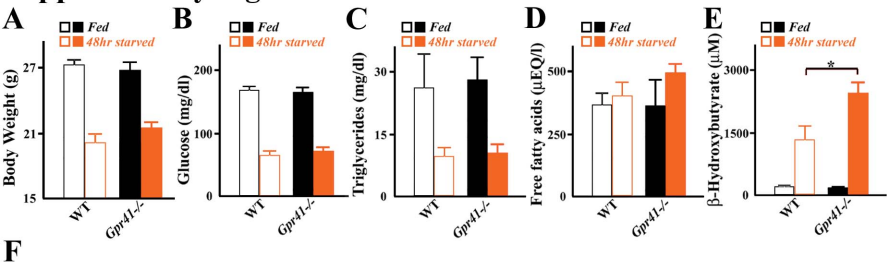
Parameter	Result for group				P value			
	WT (Control)	Gpr41-/- (Control)	WT (Diabetes)	Gpr41-/- (Diabetes)	Control (WT vs Gpr41-/-)	Diabetes (WT vs Gpr41-/-)	WT (Control vs Diabetes)	Gpr41-/- (Control vs Diabetes)
Heart Rate (beat/min)	708 ± 5.8	663 ± 3.1	403 ± 38	546 ± 25	$p < 0.005$ **	$p < 0.05$ *	$p < 0.005$ **	$p < 0.005$ **
Body wt (g)	28.1 ± 0.8	29.0 ± 0.7	22.7 ± 0.7	23.9 ± 0.9	$p > 0.05$	$p > 0.05$	$p < 0.005$ **	$p < 0.005$ **
Plasma Glucose (mg/dl)	162 ± 8.3	169 ± 3.5	512 ± 53	495 ± 82	$p > 0.05$	$p > 0.05$	$p < 0.005$ **	$p < 0.005$ **
Plasma β-Hydroxybutyrate (mM)	0.10 ± 0.04	0.06 ± 0.03	2.62 ± 0.7	2.40 ± 0.4	$p > 0.05$	$p > 0.05$	$p < 0.005$ **	$p < 0.005$ **

Supplementary Figure 9